Phytochemistry 166 (2019) 112060

Contents lists available at ScienceDirect

Phytochemistry

journal homepage: www.elsevier.com/locate/phytochem

Alkaloids isolated from *Tabernaemontana bufalina* display xanthine oxidase inhibitory activity

Bao-Bao Shi[a,b], Jing Chen[a,b], Mei-Fen Bao[a,b], Ying Zeng[a,c,**], Xiang-Hai Cai[a,c,*]

[a] State Key Laboratory of Phytochemistry and Plant Resources in West China, Kunming Institute of Botany, Chinese Academy of Sciences, Kunming, 650201, People's Republic of China

[b] University of Chinese Academy of Sciences, Beijing, 100049, People's Republic of China

[c] Yunnan Key Laboratory of Natural Medicinal Chemistry, Kunming, 650201, People's Republic of China

ARTICLE INFO

Keywords:
Tabernaemontana bufalina apocynaceae
Alkaloid
Taberhaines A–D
Apparicine
Xanthine oxidase inhibitor

ABSTRACT

Continued interest in bioactive alkaloids led to the isolation of four undescribed alkaloids along with 74 known ones from the aerial parts of *Tabernaemontana bufalina* Lour. The structures of the yet undescribed alkaloids were elucidated based on NMR, IR, UV, MS and CD spectroscopic data and X-ray crystal diffraction and, according to the plant source, named as taberhaines A–D (**1**–**4**). The known compounds comprised of 66 monoterpenoid indole, three carboline and five isoquinoline alkaloids. Among them, the known apparicine inhibited significantly the activity of xanthine oxidase, which plays an important role for gout, with an IC_{50} value of 0.65 μM, compared to the standard drug allopurinol (IC_{50} = 0.60 μM).

1. Introduction

The sickness gouty arthritis or gout is caused by deposition of sodium urate (SU) crystals within joints in the setting of chronic hyperuricaemia. It presently becomes the most common type of arthritis worldwide. When the sodium urate concentration in the blood serum is lower than the saturation point of SU, the formation of new crystals is prevented and existing crystals can be dissolved. Thus, keeping SU below the saturation point in the blood serum is a key process in the treatment of Gout. Currently, uricosuric drugs like probenecid and benzbromarone (Bach and Simkin, 2014) and the anti-inflammatory agents colchicine and loxoprofen sodium (Pascart and Richette, 2018; Greig and Garnock-Jones, 2016) are used for treating this sickness. Concerning the formation of SU, the enzyme Xanthine oxidase (XO) plays an important role (Pacher et al., 2006). According to Delgado et al. (1966) and Bruce (2006) inhibition of XO by using allopurinol or febuxostat decreases the concentration of SU in the blood serum. However, the existing first-line drugs were reported to have cardiotoxic effects (Krishnamurthy et al., 2015). Hence, the search for new candidates with XO inhibition activities became already a hotspot in gout drug research. Natural products were proved to be a good resource of novel drugs, thus we tried to find novel potential compounds from plant species. So According to Mehmood et al. (2019), XO inhibitors from plants are belonging to various classes of compounds, like flavonoids, saponins, terpenoids, isoquinines and also simple indoles. The fact, that isoquinines and simple indole of the above-mentioned drugs contain nitrogen, prompted us to search for plant-derived alkaloids. As part of our ongoing research for bioactive monoterpenoid indole alkaloids (MIAs), a phytochemical study combined with screening for biological activities on *Tabernaemontana bufalina* Lour., a rich resource of structurally diverse MIAs, was carried out. The present paper describes the isolation and xanthine oxidase inhibition activities of 78 alkaloids including four new ones (Fig. 1) from this plant species.

2. Results and discussion

Chromatographic separation of the alkaloid fraction of *T. bufalina* yielded a total of 78 compounds (section 3). All compounds exhibited positive reactions with Dragendorff's reagent on TLC plates.

Alkaloid **1** was obtained as a yellow powder and showed UV absorptions at 198, 229, and 329 nm. The ^{13}C NMR data of **1** indicated a glucoside moiety [δ_C 100.3 (d), 78.4 (d), 74.6 (d), 71.5 (d), 77.9 (d), 62.7 (t)]. In addition, a terminal double bond [δ_C 119.1 (t), 135.9 (d)], an α, β-unsaturated carboxylic methyl ester [δ_C 154.5 (d), 109.0(s),

* Corresponding author. State Key Laboratory of Phytochemistry and Plant Resources in West China, Kunming Institute of Botany, Chinese Academy of Sciences, Kunming, 650201, People's Republic of China.

** Corresponding author. State Key Laboratory of Phytochemistry and Plant Resources in West China, Kunming Institute of Botany, Chinese Academy of Sciences, Kunming, 650201, People's Republic of China.

E-mail addresses: biochem@mail.kib.ac.cn (Y. Zeng), xhcai@mail.kib.ac.cn (X.-H. Cai).

https://doi.org/10.1016/j.phytochem.2019.112060
Received 15 April 2019; Received in revised form 19 June 2019; Accepted 26 June 2019
Available online 11 July 2019
0031-9422/

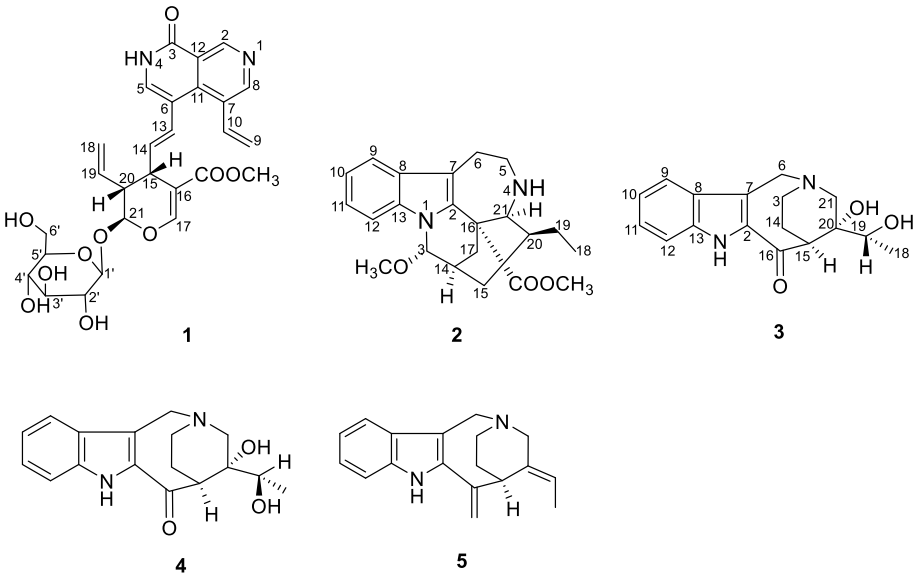

Fig. 1. Undescribed and active alkaloids (**1–4**) isolated from *T. bufalina*. Appricine = **5**.

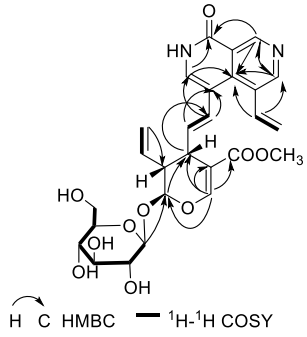

Fig. 2. Key HMBC, and ^{1}H-^{1}H COSY correlations of **1**.

168.7 (s), 51.8 (q)], two methines (δ_C 39.7 and 46.6) and the glucose unit support the existence of a secologanin analogue. Both coupled double bond signals of δ_H at 6.63 (J = 15.3 Hz, H-13) and at 5.77 (J = 15.3 Hz, H-14) showed HMBC correlations to C-15 (δ_C 39.7 d), accounting for the missing aldehyde signal of secologanin in the ^{1}H and ^{13}C NMR spectrum. The secologanin unit was further supported by the ^{1}H-^{1}H COSY correlations of H-18/19/20/15/14/13 and the HMBC correlations as shown in Fig. 2. Lastly, the remaining sp^2 ^{13}C NMR signals (δ_C 151.0 (d), 150.8 (d), 133.4 (d), 163.5 (s), 141.6 (s), 136.3 (d), 132.4 (s), 121.7 (s), 116.7 (s), 119.0 (t)] of **1** suggested the existence of a gentianine analogue (Bailleul et al., 1977) except the absence of two sp^3 signals in **1**. However, the molecular formula $C_{27}H_{30}N_2O_{10}$ of **1** deduced from the negative HRESIMS (m/z 541.1826, [M - H]$^-$), disclosed the presence of another *N* atom. Further, ^{13}C NMR comparison of **1** with gentianine, showed the chemical shifts at δ_C 133.4 (C-5, d) of **1**. This signal fitted better to a -NH-CH=C than to a -O-CH=C unit. The correlations from H-13 to C-5, and C-6 (δ_C 116.7, s) in the HMBC spectrum indicated, that both units were connected via C-6/13. The geometry of the double bond of C-13/14 was determined as *E* by their coupling constant (J = 15.3 Hz). Likewise, the J values (J = 7.9 Hz) of the anomeric proton revealed a β-configuration of the glucose residue. The stereo-configuration of **1** remained identical to the secologanin moiety since no bond break during biosynthesis occurred. Based on these data, the structure of **1** was elucidated.

The IR absorption bands of alkaloid **2** at 3437, 1715, 1602, 1491 cm^{-1} suggested the presence of NH, C=O, and benzene rings, which are characteristic functionalities of MIAs. The UV absorption bands at 226 and 283 nm were also in agreement to these alkaloids. Alkaloid **2** possesses a molecular formula $C_{22}H_{28}N_2O_3$ as established by the HRESIMS m/z 369.2175 [M + H]$^+$ and ^{13}C NMR spectroscopic data, indicating 10 degrees of unsaturation. The ^{1}H NMR spectra of **2** exhibited two doublets [δ_H 7.40 (2H, *d*, J = 7.9 Hz, H-9, 12)] and two triplets [(δ_H 7.08 (1H, t, J = 7.9 Hz, H-11), 7.03 (1H, t, J = 7.9 Hz, H-10)], in association with an A-ring unsubstituted indole. Its ^{13}C and DEPT spectra (Table 1) showed 22 carbon resonances due to six quaternary carbons (δ_C 176.6, 138.8, 133.0, 130.1, 109.9, 50.1), eight methines (δ_C 118.5, 120.5, 121.8, 110.5, 87.6, 31.8, 36.7, 58.8), five methylenes (δ_C 41.0, 23.6, 25.1, 24.7, 24.6), two methoxyls (δ_H 55.9, 52.6), and one methyl group (δ_C 12.6). Above-mentioned ^{13}C NMR pattern of **2** was identical to those of coronaridine (Pereira et al., 2008), except that a NCH$_2$ ab. δ_C 50 in the latter compound was substituted by a NCH group, which gave a signal at δ_C 87.6 in **2**. The corresponding proton signal of the new methine showed HMBC correlations to C-13, C-2 and methoxyl (δ_C 55.9), confirming the linkage of N$_1$-CH-OMe. Careful analysis suggested this methine should be CH-3. Its absolute configuration (3*S*,14*R*,16*S*,20*S*,21*S*) was identical to its precursor, coronaridine, and confirmed by Cu Kα X-ray diffraction (Flack parameter of 0.04(4)) (Fig. 3). The H-15 in this rigid molecule gave a resonance at δ_H 0.30 which may be caused by its anisotropy.

The molecular formula of both compounds **3** and **4** were determined as $C_{17}H_{20}N_2O_3$ by HRESIMS and ^{13}C NMR data, indicating nine indices of hydrogen deficiency. Their UV spectrum showed absorption maxima at 235 and 312 nm, which are characteristic for a 2-acylindole chromophore. The ^{1}H NMR spectrum of **3** showed signals of an indole ring [δ_H 7.59 (d, J=8.1 Hz)], [δ_H 7.03 (t, J = 8.1 Hz)], [δ_H 7.26 (t, J = 8.1 Hz)], [δ_H 7.50 (d, J = 8.1 Hz)], and a hydroxyethyl side chain [δ_H 3.68 (1H, q, J = 6.4 Hz, H-19) and 1.20 (3H, d, J = 6.4 Hz, H-18)]. A single methylene was assigned CH$_2$-6 from the characteristic self-couple signals [δ_H 4.84 (1H, d, J = 18.1 Hz) and 4.43 (1H, *d*, J = 18.1 Hz)], and their HMBC correlation to C-8/2. The six remaining carbon signals, including one carbonyl [δ_C 193.8 (s)], three methylenes (δ_C 56.7, 53.9 and 43.3), and a quaternary carbon [δ_C 74.9 (s)] further suggested that **3** possess structural similarities to conolobine A/B (Kam et al., 2004). Latter compound possesses a 19,20-epoxy group whilst in **3** a 19,20-diol is present. Further, the HMBC correlations of H-18/C-20, H-21/C-19 and H-15/C-19 confirmed this -diol group.

Compound **4** showed almost identical ^{13}C NMR spectra as compound **3**. Analyses of the 1D and 2D NMR data (^{1}H-^{1}H COSY, HSQC, and HMBC) confirmed that both compounds possess the same planar

Table 1
^{1}H and ^{13}C NMR Spectroscopic Data for **1–4** in acetone-d_6 (δ in ppm, J in Hz).

entry	δ_H (1)[a]	δ_C (1)[b]	δ_H (2)[a]	δ_C (2)[b]	δ_H (3)[a]	δ_C (3)[b]	δ_H (4)[a]	δ_C (4)[b]
2	9.31 (s)	150.8 d		133.0 s		133.5 s		133.5 s
3		163.5 s	5.08 (d, 1.9)	87.6 d	3.19 (ddd,13.7, 9.5, 2.4) 3.05 (ddd,13.7, 8.9, 2.4)	43.3 t	3.18 (ddd, 13.6, 9.1, 2.5) 3.08 (ddd, 13.6, 8.7, 2.5)	43.3 t
5	7.21 (s)	133.4 d	3.05 (m) 2.54 (m)	41.0 t				
6		116.7 s	2.57 (m) 2.79 (m)	23.6 t	4.84 (d, 18.1) 4.43 (d, 18.1)	53.9 t	4.82 (d, 18.2) 4.43 (d, 18.2)	53.9 t
7		132.4 s		109.9 s		120.7 s		120.7 s
8	8.57 (s)	151.0 d		130.1 s		128.6 s		128.5 s
9	5.29 (d, 17.2) 5.22 (d, 11.0)	119.0 t	7.40 (d, 7.9)	118.5 d	7.59 (d, 8.1),	121.2 d	7.59 (d, 8.1),	121.2 d
10	7.34 (dd, 17.2, 11.0)	136.3 d	7.03 (t, 7.9)	120.5 d	7.03 (t, 8.1)	112.8 d	7.03 (t, 8.1)	112.8 d
11		141.6 s	7.08 (t, 7.9)	121.8 d	7.26 (t, 8.1)	125.9 d	7.26 (t, 8.1)	126.0 d
12		121.7 s	7.40 (d, 7.9)	110.5 d	7.50 (d, 8.1)	120.0 d	7.50 (d, 8.1)	120.0 d
13	6.63 (d, 15.3)	131.2 d		138.8 s		137.4 s		137.5 s
14	5.77 (t, 15.3)	131.7 d	2.64 (m)	31.8 d	2.04 (m) 1.81 (m)	23.2 t	1.89 (m) 1.82 (m)	22.7 t
15	3.79 (dd, 15.3, 8.2)	39.7 d	1.53 (m) 0.30 (td, 14.0, 7.0)	25.1 t	3.32(dd, 6.3, 2.3)	54.9 d	3.56 (dd, 5.7, 2.4)	52.8 d
16		109.0 s		50.1 s		193.8 s		194.0 s
17	7.60 (s)	154.5 d	2.35 (d, 13.0) 1.93 (dd, 13.0, 5.4)	24.7 t				
18	5.61 (d, 17.2) 5.41 (d, 11.0)	119.1 t	0.86 (t, 7.2)	12.6 q	1.20 (d, 6.4)	17.2 q	1.16 (d, 6.3)	16.5 q
19	5.80 (m)	135.9 d	1.34 (m) 0.95 (m)	24.6 t	3.68 (q, 6.4)	74.9 t	3.66 (q, 6.3)	71.7 t
20	2.67 (dd, 13.8, 8.2)	46.6 d	1.84 (m)	36.7 d		74.9 s		75.3 s
21	5.54 (d, 7.9)	97.6 d	3.83 (d, 7.1)	58.8 d	3.48 (d, 15.2) 2.96 (d, 15.2)	56.7 t	3.29 (d, 15.2) 2.90 (d, 15.2)	57.5 t
OCH_3			3.54 (s)	55.9 q				
$\underline{C}OOCH_3$		168.7 s		176.6 s				
$COO\underline{C}H_3$		51.8 q	3.62 (s)	52.6 q				
1′	4.69 (d, 7.9)	100.3 d						
2′	3.16 (m)	74.6 d						
3′	3.30 (m)	78.4 d						
4′	3.21 (m)	71.5 d						
5′	3.32 (m)	77.9 d						
6′	3.83 (m) 3.55 (m)	62.7 t						

[a] Recorded at 400 MHz.
[b] Recorded at 125 MHz. Compound **1** was recorded in CD_3OD

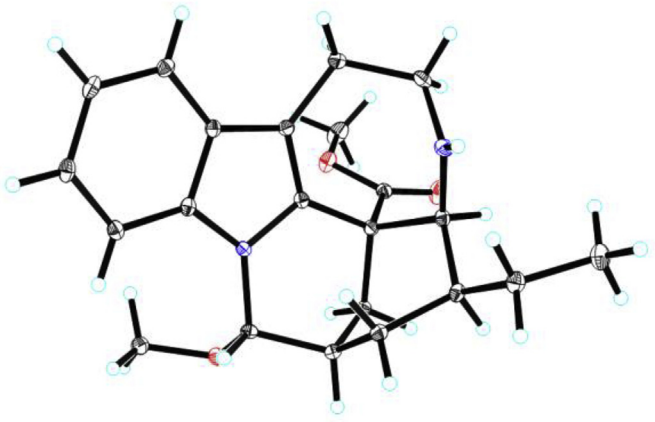

Fig. 3. The X-ray crystal structure of **2**.

structure and were epimers.

The absolute configuration of the 19,20-diol moiety in **3** and **4** were assigned using the in situ dimolybdenum CD method developed by Snatzke and Frelek (Bari et al., 2001). Upon addition of dimolybdenum tetraacteate [$Mo_2(OAc)_4$] to **3** and **4** in DMSO solution, a metal complex of chiral *vic*-diol with the achiral $Mo_2(OAc)_4$ was generated, which possesses an auxiliary chromophore. Compounds **3** and **4** showed identical CD spectra resulting from the C-16 ketone chromophore. After recording the CD spectra, this contribution was subtracted to give the induced CD of the metal complex which finally avoid its overlap (> 250 nm). Therefore, the observed sign of the Cotton effect in the induced spectrum originates solely from the chirality of the *vic*-diol moiety expressed by the sign of the O-C-C-O torsion angle. The negative Cotton effects observed at around 310 nm in the induced CD spectrum (Fig. 4) permitted assignment of the 19*R* and 20*R* absolute configuration on basis of the empirical rule proposed by Snatzke, with the bulkier benzyl group pointing away from the remaining portion of the complex. Considering the relative configuration established by NOESY data, absolute configuration of **3** was assigned as 15*S*, 19*R*, 20*R* based on the negative sign at 317 nm. On the contrary, the absolute configuration of **4** was assigned as 15*S*, 19*S*, 20*R* by the positive sign at 313 nm. This presumption was further supported by the observed NOEs between H-19/H-21 and H-18/H-15, and the absence of NOEs between H-19/H-15 and H-18/H-21 (Fig. 5). It is noteworthy, that the chemical shift of H-15 in **4** was relatively deshielded (δ 3.56) compared to the chemical shift of H-15 in the 19(*R*)-epimer **3** (δ 3.32). This was attributed to paramagnetic deshielding caused by the proximity of the OH oxygen atom to H-15, which was only possible if rotation about the C-19-C-20 bond was indeed restricted (Fig. 5). Taking its biogenesis into account, the 19-OH configurations was likely to be inverse, which would be consistent with the anticipated, less hindered hydrolytic decomposition of the precursor epoxide.

The known alkaloids were identified as apparicine (**5**) (Van Beek et al., 1984), conolobine (**6**) (Kam et al., 2004), conolobine (**7**) (Kam

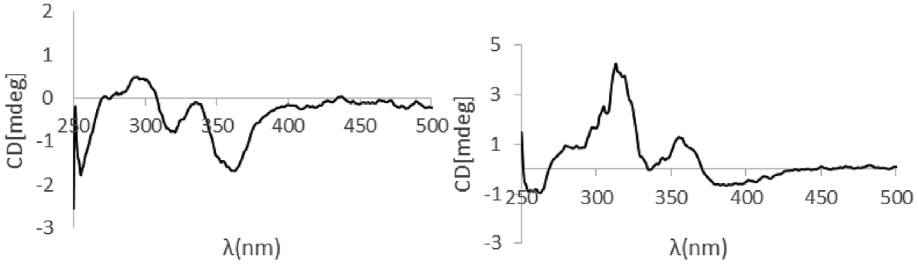

Fig. 4. CD spectra of in situ formed Mo-complexes of **3** and **4** containing $Mo_2(OAc)_4$ with the inherent CD spectra subtracted.

et al., 2004), o-acetyl-vallesamine (**8**) (Perera et al., 1984), vallesamine (**9**) (Perera et al., 1984), conolidine (**10**) (Kam et al., 2004), coronaridinehydroxyindolenine (**11**) (Sharma and Cordell, 1988), heyneanine hydroxyindolenine (**12**) (Monique et al., 1995), voaphylline (**13**) (Kunesch and Tulinsky, 1967), velbanamine (**14**) (Wenkert et al., 1976), voacangine (**15**) (Okuyama et al., 1992), coronaridine (**16**) (Pereira et al., 2008), 10-hydroxycoronaridine (**17**) (Kutney et al., 1978), taberdivarine G (**18**) (Zhang et al., 2015a), 3-oxocoronaridine (**19**) (Sharma and Cordell, 1988), ervatamine I (**20**) (Zhang et al., 2015b), heyneanine (**21**) (Gunasekera et al., 1980), ervatamine H (**22**) (Zhang et al., 2015b), 3-(2-oxopropyl)-coronaridine (**23**) (Ahond et al., 1976), 10-hydroxyheyneanine (**24**) (Schripsema et al., 1986), voacristine (**25**) (Wenkert et al., 1979), 3-ketopropyl-19*R*-heyneanine(**26**) (Perera et al., 1985), 19*S*-hydroxyibogamine (**27**) (Kam and Sim, 2002), pseudoindoxyl coronaridine (**28**) (Rastogi et al., 1980), ervatamine F (**29**) (Zhang et al., 2015b), isovallesiachotamine (**30**) (Waterman and Zhong, 1982), vallesiachotamine (**31**) (Waterman and Zhong, 1982), ajmalicine (**32**) (Höfle et al., 1980), tetrahydroalstonine (**33**) (Höfle et al., 1980), vallesiachotamine (**34**) (Waterman and Zhong, 1982), 10-hydroxyAntirhine (**35**) (Boughandjioua et al., 1989), antirhine (**36**) (Boughandjioua et al., 1989), vobasine (**37**) (Clivio et al., 1990), 16-epivobasine (**38**) (Clivio et al., 1990), isositsirikine (**39**) (Kutney and Brown, 1966), geissoschizol (**40**) (Feng et al., 1982), 10-hydroxygeissoschizol (**41**) (Feng et al., 1982), rhazimal (**42**) (Atta-ur-Rahaman and Habib-ur-Rehman, 1986), 16-epiakuammiline (**43**) (Subramaniam et al., 2007), strictamine (**44**) (Atta-ur-Rahaman and Habib-ur-Rehman, 1986), vincophylline (**45**) (Subramaniam et al., 2007), rhazimine (**46**) (Hu et al., 1987), meloyine (**47**) (Zhang et al., 2017), apogeissoschizin (**48**) (Aimi et al., 1977), normacusine B (**49**) (Yu et al., 2003), lochnerine (**50**) (Mors et al., 1956), pachysipine (**51**) (Zhou et al., 2012), pseudovincadifformine(**52**) (Kalaus et al., 1993), epipseudovincadifformine (**53**) (Kalaus et al., 1993), pandine (**54**) (Le Men et al., 1974), pandoline (**55**) (Kan et al., 1981), fluorocarpamine (**56**) (Atta-ur-Rahaman et al., 1989), tubotaiwine (**57**) (Baassou et al., 1978), 19*R*-methoxytubotaiwine (**58**) (Lim et al., 2007), tribulusterine (**59**) (Ying et al., 2013), 14,15-didehydro-10,11-dimethoxy-16-epivincamine (**60**) (Zhang et al., 2007), 14,15-didehydro-10-hydroxy11-methoxy-16-epivincamine (**61**) (Zhang et al., 2007), 14,15-didehydro-10-hydroxy11-methoxy-16-epivincamine (**62**) (Zhang et al., 2007), 14,15-didehydro-10,11-dimethoxyvincamine (**63**) (Zhang et al., 2007), epi-dehydrovincamine (**64**) (Zhang et al., 2003), carbazoline (**65**) (Leonard and Elderfield, 1942), deoxyvasicinone (**66**) (Al-Shamma et al., 1981), aspidospermidine (**67**) (Eles et al., 2002), conophylline (**68**) (Kam et al., 2003), conophyllidine (**69**) (Kam et al., 1993), ervahanine C (**70**) (Feng et al., 1981), conodurine (**71**) (Kam and Sim, 2003), ervahanine A (**72**) (Kam and Sim, 2003), alstrostine A (**73**) (Cai et al., 2011), przewalskine (**74**) (Mollov and Le, 1971), przewalskine (**75**) (Zhang et al., 1998), stebisimine (**76**) (Matsui et al., 1982), micheline B (**77**) (Chen et al., 1997), N-oxyoliveroline (**78**) (Hamonniere et al., 1977) based on their NMR spectra.

Alkaloids **2–6**, **9–11**, **16–22**, **24**, **26**, **28**, **37–38**, **42–44**, **53–55**, **60–63**, **67–69**, **73** and **78** were screened for the xanthine oxidase inhibitory activities, with allopurinol as positive control. The inhibition activities of **3**, **4**, **5**, **18**, **24**, **37**, **55** and **68** were shown in Table 2. Among them, alkaloid **5** showed a significant xanthine oxidase inhibitory activity with an IC_{50} value of 0.65 μM, whereas the IC_{50} value

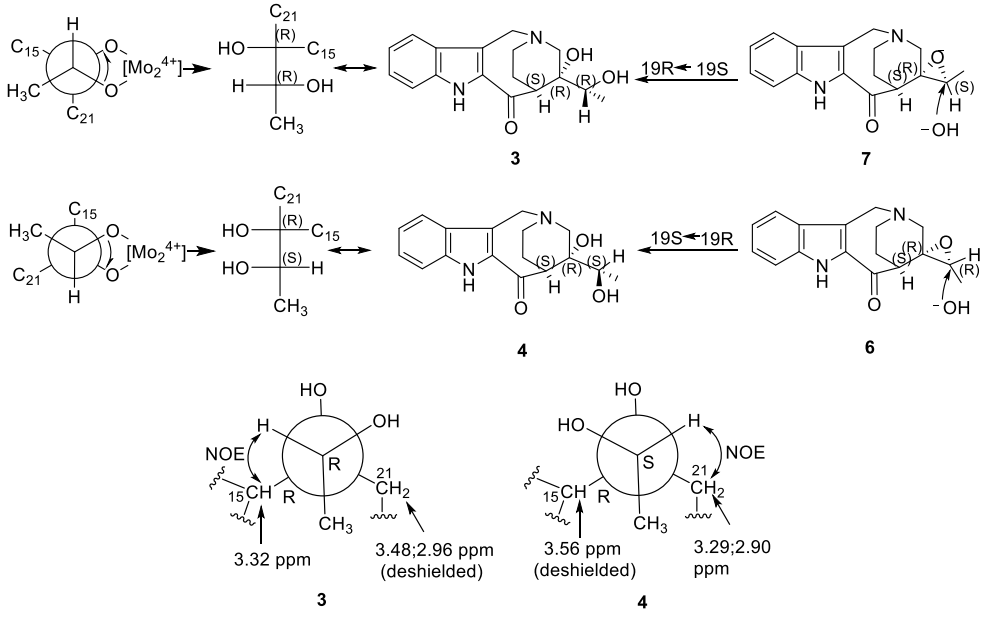

Fig. 5. Biosynthesis and stereochemical analysis of **3** and **4**.

Table 2
Xanthine oxidase inhibition activity of alkaloids **3**, **4**, **5**, **18**, **24**, **37**, **55**, **68** and allopurinol.

Compound	ICB_{50B} (μM)
3	43.67
4	34.34
5	0.65
18	6.50
24	16.54
37	10.21
55	8.52
68	6.83
Allopurinol	0.60

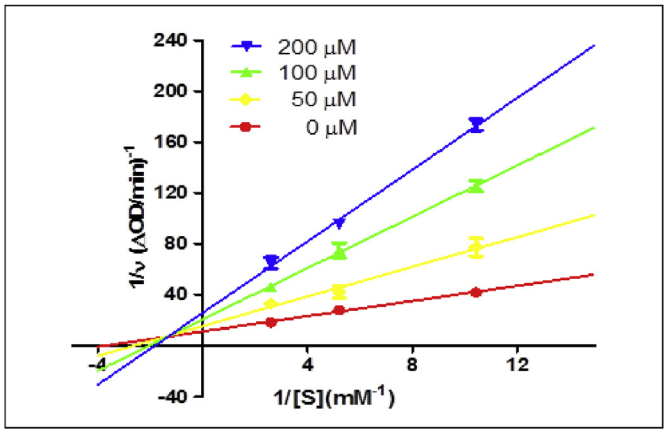

Fig. 6. Lineweaver-Burk plots in the absence or at the different concentrations of compound **5**.

of the positive control allopurinol was 0.60 μM. To understand the enzyme inhibition mode of compound **5**, Lineweaver-Burk plots were established, as shown in Fig. 6. The calculated curve of compound **5** in the Lineweaver-Burk plots cross the 1/V axis in the positive range and the 1/[S] axis in the negative range. These characteristics are specific for a mixed type of inhibition. From the secondary plots of Lineweaver-Burk curves, K_i and K_{is} were calculated to be 55.11 and 155.07 μM, respectively. The K_i value was lower than K_{is},which indicates that compound **5** tends to be easily and firmly bound to the free XO rather than to the xanthine-XO complex.

Autodock vina 4.0 was selected as the docking software to investigate the binding mode between compound **5** and XO. As shown in Fig. 7, compound **5** occupied the hydrophobic pocket composed by the amino acids Leu1014, Val1011, Lys771, Leu873, Leu648, Phe649, His875, Glu879, Ser876, Pro1076, which form strong hydrophobic bonds. Since the results of the molecular docking simulation were in good accordance with the above-mentioned experimental results, we infer that compound **5** may fill the narrow channel leading to the molybdenum center of XO. This effect leads finally to the inhibition of this enzyme.

3. Conclusion

As a result of a systematic examination of the alkaloidal fraction from the plant species *T. bufalina*, 78 alkaloids were identified. The previously described compound, apparicine (**5**) (Van Beek et al., 1984) showed strong inhibitory effects of xanthine oxidase, with an IC_{50} of 0.65 μM, almost equivalent to that of the reference compound, allopurinol. It could be shown, that inhibition is caused by a mixed mode.. Docking studies indicated, numerous of strong hydrophobic bonds are formed between compound **5** and the active site residues of the enzyme.Hence, compounds **5** is blocking the narrow channel leading to the molybdenum center of the enzyme. Thus, **5** represents a promising lead structure for the further exploration of xanthine oxidase inhibitors.

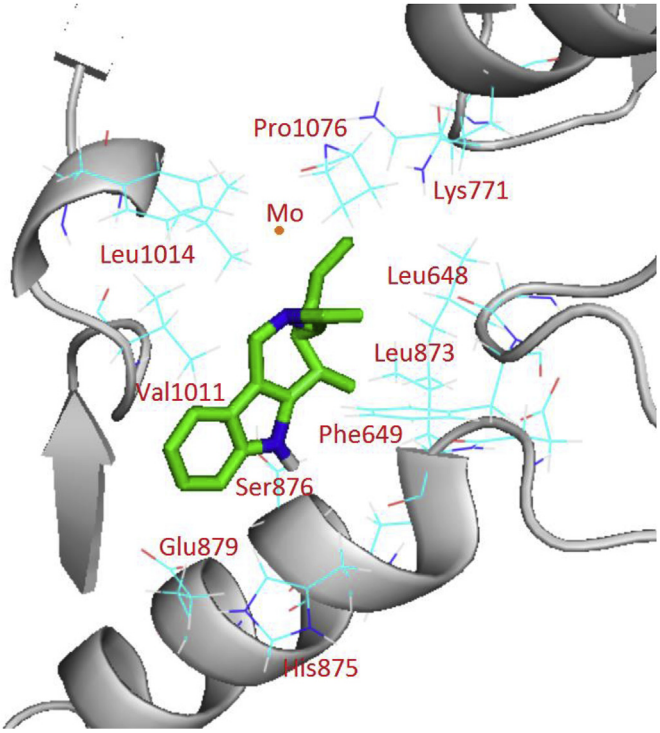

Fig. 7. Active site of xanthine oxidase (1N5X) complexed with compound **5**.

4. Experimental

4.1. General experimental procedures

Optical rotations were measured on a Jasco p-1020 digital polarimeter. UV spectra were recorded on a Shimadzu 2401A spectrophotometer. IR spectra were obtained on a Bruker Tensor 27 infrared spectrophotometer with KBr pellets. X-ray data was determined using a Bruker APEX DUO instrument. ^1H, ^{13}C and 2D NMR spectra were obtained on Bruker AVANCE III-400, 500 and 600 MHz spectrometers with $SiMe_4$ as an internal standard. ESI- and HRESIMS data were recorded on a Bruker HCT/Esquire and an Agilent G6230 TOF MS. CD spectra were obtained on a Chirascan V100 spectrometer (Applied Photophysics, Surrey, UK). Column chromatography (CC) (200 × 1500, 26 × 254, 20 × 203, and 13.4 × 203 mm, respectively) was performed on either silica gel (200–300 mesh, Qing-dao Haiyang Chemical Co., Ltd., Qingdao, China) or RP-18 silica gel (20–45 μm, Fuji Silysia Chemical Ltd., Japan). Fractions were monitored by TLC on silica gel plates (GF254, Qingdao Haiyang Chemical Co., Ltd., Qingdao, China), and spots were visualized with Dragendorff's reagent. MPLC was performed using a Buchi pump system coupled with RP-18 silica gel-packed glass columns (15 × 230, 26 × 460, and 70 × 460 mm, respectively). HPLC was performed using Waters 1525E pumps coupled with analytical semi-preparative or preparative Sunfire C_{18} columns (5 μm, 4.6 × 150, and 19 × 250 mm, respectively). The HPLC system employed a Waters 2998 photodiode array detector and a Waters fraction collector III.

4.2. Plant material

Leaves and twigs of *Tabernaemontana bufalina* Lour. (Apocynaceae) were collected in Feb. 2017 during the dry season in Changjiang, Hainan Province, P. R. China, and identified by Dr. Sheng-Zhuo Huang. A voucher specimen (No. Cai20170220) was deposited in the State Key

Laboratory of Phytochemistry and Plant Resources in West China, Kunming Institute of Botany, Chinese Academy of Sciences.

4.3. Extraction and isolation

Air-dried branches and leaves of T. *bufalina* (48 kg) were powdered and extracted with MeOH (96 L × 3) at room temperature for a week, the solvent was removed *in vacuo*. The extract (2.3 kg) was partitioned between 0.5% HCl solution and EtOAc, and the acidic water layer was afterwards adjusted to pH 8–9 with 15% ammonia solution and subsequently extracted with EtOAc. This yielded 180 g crude alkaloid extract. This extract was subjected to column chromatography (CC) over silica gel and eluted with gradient $CHCl_3$-Me_2CO (1:0–1:1, v/v) to afford seven fractions (I-VII).

Fraction I (5.6 g) was further chromatographed on a C_{18} MPLC column eluted with a gradient of MeOH-H_2O (30:70-100: 0, v/v) to give the five subfractions I-1-I-5. Subfraction I-3 (1.9 g) was subjected to C_{18} MPLC column once again using MeOH-H_2O (50:50-80:20, v/v) as eluent to give the five subfractions (I-3-1 ~ I-3-5). Fraction I-3-1 was further purified by a preparative column with a gradient flow from 50% to 65% aqueous methanol to give **6** (10.0 mg), **7** (4.5 mg), **15** (21.0 mg), **16** (35.5 mg). Fraction I-3-2 was purified by a preparative C_{18} HPLC column with a gradient of MeOH-H_2O (55:45-70:30, v/v) to obtain **11** (7.8 mg), **17** (10.3 mg), and **26** (6.2 mg). I-4 (1.0 g) was separated using C_{18} MPLC column with a gradient of MeOH-H_2O (50:50-80:20, v/v) to afford three subfractions (I-4-1 ~ I-4-3). Fraction (I-4-2) was purified by a preparative C_{l8} HPLC column with a gradient of MeOH-H_2O (60:40-75:25, v/v) to obtain **67** (4.5 mg), **18** (20.5 mg), **19** (11.4 mg), **51** (3.4 mg).

Fraction II (10.2g) was chromatographed on a C_{18} MPLC column eluted with a gradient of MeOH-H_2O (30:70-100:0, v/v) to give the four subfractions II-1 ~ II-4. Subfraction II-2 (3.2g) was subjected to C_{18} MPLC column again using MeOH-H_2O (40:60-80:20, v/v) as eluent to give the three subfractions (II-2-1 ~ II-2-3). Fraction II-2-1 was further purified by a preparative column with a gradient flow from 50% to 65% aqueous methanol to give **20** (4.3 mg), **55** (26.5 mg). Fraction II-2-2 was purified by a preparative C_{18} HPLC column with a gradient of MeOH-H_2O (55:45-70:30, v/v) to obtain **32** (7.8 mg), **33** (10.3 mg), **53** (3.8 mg) and **52** (6.2 mg). II-3 (2.9 g) was separated using C_{18} MPLC column with a gradient of MeOH-H_2O (40:60-80:20, v/v) to afford four subfractions (II-3-1 ~ II-3-4). Fraction II-3-2 was purified by a preparative C_{18} HPLC column with a gradient of MeOH-H_2O (60:40-75:25, v/v) to obtain **30** (4.5 mg), **12** (20.5 mg), **37** (11.4 mg).

Fraction III (8.9 g) was fractionated by C_{18} MPLC column with a gradient of MeOH-H_2O (10:90-100:0, v/v) to give four subfractions (III-1 ~ III-4). Fraction III-1 was separated using a Sephadex LH-20 column eluted with MeOH. Four subfractions (III-1-1 to III-1-4) were collected. III-1-2 was purified using a preparative C_{18} HPLC column with a gradient of MeCN-H_2O (40:60-55:45, v/v) to obtain **54** (18.8 mg), **21** (13.5 mg), **66** (1.9 mg). III-2 (3.5 g) was separated using C_{18} MPLC column with a gradient of MeOH-H_2O (40:60-80:20, v/v) to afford three subfractions (III-2-1 ~ III -2-3). Fraction III-2-2 was purified by a preparative C_{18} HPLC column with a gradient of MeCN-H_2O (40:60-55:45, v/v) to obtain **13** (1.5 mg), **22** (15.8 mg), **10** (18.1 mg), **38** (7.6 mg), **23** (20.5 mg).

Fraction IV (13.6 g) was fractionated by C_{18} MPLC column with a gradient of MeOH-H_2O (10:90-100:0, v/v) to give five subfractions (IV-1 ~ IV-5). Fraction IV-1 was purified by a preparative C_{18} HPLC column with a gradient of MeCN-H_2O (30:70-45:55, v/v) to obtain **69** (7.8 mg), **65** (5.3 mg), **59** (2.2 mg). Fraction IV-2 was separated using a Sephadex LH-20 column eluted with MeOH. Three subfractions (IV-2-1 to IV-2-3) were collected. IV-2-1 was purified by a preparative C_{18} HPLC column with a gradient of MeCN-H_2O (40:60-55:45, v/v) to obtain **60** (3.6 mg), **61** (3.1 mg), **62** (5.6 mg). IV-2-2 was purified by a preparative C_{18} HPLC column with a gradient of MeCN-H_2O (45:55-60:40, v/v) to obtain **8** (3.6 mg), **2** (3.1 mg), **56** (5.6 mg), **24** (35.1 mg).

Fraction V (8.5 g) was fractionated by C_{18} MPCL column with a gradient of MeOH-H_2O(10:90-100:0, v/v) to give four subfractions (V-1 ~ V-4). Fraction V-2 (2.5g) was separated using a Sephadex LH-20 column eluted with MeOH. Four subfractions (V-2-1 ~ V-2-4) were collected. V-2-1was purified by a preparative C_{l8} HPLC column with a gradient of MeCN-H_2O (30:70-45:55, v/v) to obtain **70** (3.1 mg), **71** (3.8 mg), **68** (9.8 mg). V-4 (3.1 g) was separated using C_{18} MPLC column with a gradient of MeOH-H_2O (40:60-100:00, v/v) to afford three subfractions (V-4-1 ~ V-4-3). Fraction V-4-2 was purified by a preparative C_{18} HPLC column with a gradient of MeCN-H_2O (35:65-50:50, v/v) to obtain **63** (2.5 mg), **48** (1.9 mg), **42** (23.5 mg), **43** (18.3 mg), **44** (15.7 mg), **45** (20.1 mg).

Fraction VI (14.5 g) was fractionated by C_{18} MPLC column with a gradient of MeOH-H_2O(10:90-100:0, v/v) to give six subfractions (VI-1 ~ VI-6). VI-1 was purified by a preparative C_{18} HPLC column with a gradient of MeCN-H_2O(20:80-35:65, v/v) to obtain **64** (1.5 mg), **25** (10.3 mg), **5** (30.2 mg), **27** (7.8 mg). Fraction VI-2 was separated using a Sephadex LH-20 column eluted with MeOH. four subfractions (VI-2-1 ~ VI-2-4) were collected. VI-2-2 was purified by a preparative C_{l8} HPLC column with a gradient of MeCN-H_2O (25:75-40:60, v/v) to obtain **72** (4.1 mg), **34** (4.3 mg), **3** (8.3 mg), **4** (8.9 mg). VI-3 (4.9 g) was separated using C_{18} MPLC column with a gradient of MeOH-H_2O (30:60-100:20, v/v) to afford three subfractions (VI-3-1 ~ VI-3-3). Fraction VI-3-2 was purified by a preparative C_{18} HPLC column with a gradient of MeCN-H_2O (20:80-35:65, v/v) to obtain **28** (2.5 mg), **57** (1.9 mg). Fraction VI-3-3 was purified by a preparative C_{18} HPLC column with a gradient of MeCN-H_2O (25:75-40:60, v/v) to obtain **29** (3.5 mg), **9** (6.8 mg), **14** (2.3 mg), **39** (15.2 mg).

Fraction VII (20.5 g) was fractionated by C_{18} MPLC column with a gradient of MeOH-H_2O(10:90-100:0, v/v) to give six subfractions (VII-1 ~ VII-6). VII-1 was separated using a Sephadex LH-20 column eluted with MeOH. four subfractions (VII-1-1 ~ VII-1-4) were collected. VII-1-1 was purified by a preparative C_{18} HPLC column with a gradient of MeCN-H_2O(15:85-30:70, v/v) to obtain **58** (1.8 mg), **47** (25.5 mg), **40** (16.4 mg). VII-2 was separated using a Sephadex LH-20 column eluted with MeOH. Three subfractions (VII-2-1 ~ VII-2-3) were collected. VII-2-1 was purified by a preparative C_{18} HPLC column with a gradient of MeCN-H_2O (15:85-30:70, v/v) to obtain **76** (6.8 mg), **41** (20.1 mg), **35** (5.8 mg), 3**50** (4.5 mg). Fraction VII-2-2 was purified by a preparative C_{18} HPLC column with a gradient of MeCN-H_2O (20:80-35:65, v/v) to obtain **46** (12.5 mg), **36** (15.2 mg). Fraction VII-3 (4.9 g) was separated using C_{18} MPLC column with a gradient of MeOH-H_2O (20:60-100:20, v/v) to afford three subfractions (VII-3-1 ~ VII-3-3). VII-3-1 was purified by a preparative C_{18} HPLC column with a gradient of MeCN-H_2O (20:80-35:65, v/v) to obtain **49** (6.6 mg), **77** (3.5 mg), **74** (8.9 mg), **75** (9.5 mg), **78** (5.6 mg), **73** (115.2 mg). Fraction VII-4 was separated using C_{18} MPLC column with a gradient of MeOH-H_2O (20:60-100:20, v/v) to afford three subfractions (VII-4-1 ~ VII-4-3). VII-4-2 was purified by a preparative C_{18} HPLC column with a gradient of MeCN-H_2O (15:85-30:70, v/v) to obtain **1** (7.6 mg), **31** (4.8 mg) .

4.3.1. Taberhaine

A ***(1)***: yellowish powder; $C_{27}H_{30}N_2O_{10}$; [α]22 D-181.9 (c, 0.10, CH_3OH); UV (CH_3OH) λ_{max} (log ε) 198 (3.65), 229 (3.49), 329 (3.03) nm; ^1H (400 Hz) and ^{13}C (125 Hz) NMR data (CD_3OD) (Table 1); Negative ESIMS *m/z* 541 $[M - H]^-$. HRESIMS (*m/z* 541.1826 $[M - H]^-$, calcd for $C_{26}H_{30}N_2O_8$ 541.1828).

4.3.2. Taberhaine

B ***(2)***: white crystal; $C_{22}H_{28}N_2O_3$; [α]22 D-150.5 (c, 0.10, CH_3OH); UV (CH_3OH) λ_{max} (log ε) 198 (3.66), 226 (3.73), 283 (3.20) nm; ^1H (400 Hz) and ^{13}C (125 Hz) NMR data (acetone-d_6) (Table 1); Positive ESIMS *m/z* 369 $[M + H]^+$. HRESIMS (*m/z* 369.2175 $[M + H]^+$, calcd for $C_{22}H_{28}N_2O_3$ 369.2173).

4.3.3. Taberhaine

***C* (3)**: yellow oil; $C_{17}H_{20}N_2O_3$; [α]22 D-98.9 (c, 0.10, CH_3OH); UV (CH_3OH) λ_{max} (log ε) 201 (3.42), 235 (3.10), 312 (3.16) nm; ^1H (400 Hz) and ^{13}C (125 Hz) NMR data (acetone-d_6) (Table 1); Positive ESIMS *m/z* 301 $[M + H]^+$. HRESIMS (*m/z* 301.1545 $[M + H]^+$, calcd for $C_{17}H_{20}N_2O_3$ 301.1547).

4.3.4. Taberhaine

***D* (4)**: yellow oil; $C_{17}H_{20}N_2O_3$; [α]22 D-166.1 (c, 0.10, CH_3OH); UV (CH_3OH) λ_{max} (log ε) 204 (3.64), 236 (3.36), 312 (3.45) nm; ^1H (400 Hz) and ^{13}C (125Hz) NMR data (acetone-d_6) (Table 1); Positive ESIMS *m/z* 301 $[M + H]^+$. HRESIMS (*m/z* 301.1548 $[M + H]^+$, calcd for $C_{17}H_{20}N_2O_3$ 301.1547).

4.3.5. X-ray crystallographic data for 2

$C_{22}H_{28}N_2O_3$, M = 368.46, a = 7.28490(10) Å, b = 8.98050(10) Å, c = 28.5567(4) Å, $\alpha = 90^\circ$, $\beta = 90^\circ$, $\gamma = 90^\circ$, V = 1868.24(4) Å^3, T = 100(2) K, space group $P212121$, Z = 4, μ(CuKα) = 0.697 mm^{-1}, 11579 reflections measured, 3341 independent reflections (R_{int} = 0.0304). The final R_1 values were 0.0364 ($I > 2\sigma(I)$). The final $wR(F^2)$ values were 0.0972 ($I > 2\sigma(I)$). The final R_1 values were 0.0366 (all data). The final $wR(F^2)$ values were 0.0975 (all data). The goodness of fit on F^2 was 1.115. Flack parameter = 0.04(4).

4.4. Xanthine oxidase inhibition activity

Alkaloids **2–6**, **9–11**, **16–22**, **24**, **26**, **28**, **37–38**, **42–44**, **53–55**, **60–63**, **67–69**, **73** and **78** were bioassayed for inhibitory activity of xanthine oxidase. The uric acid production was calculated according to the increasing absorbance at 290 nm. Test solutions (final concentration 50 μg/mL) were prepared by adding xanthine (final concentration 29.2 μg/mL). The reaction was started by adding 40 μL of xanthine oxidase (0.1 U/mL) in a phosphate buffer solution (pH = 7.50, 0.2 mM). Alkaloids were dissolved in DMSO and immediately diluted with phosphate buffer solution to a conc of 0.5 mg/mL. The obtained mixture (total 100 μL) was incubated at 37 °C. The uric acid production was calculated from the absorbance differences to the blank solution. A test mixture without alkaloids was prepared to measure the total uric acid production. Different concentrations of alkaloids were analyzed, and then the half-maximal inhibitory concentration (IC_{50}) was calculated by linear regression analysis. Different concentrations of allopurinol were measured in triplicate.

4.5. Docking studies

Molecular docking was performed on AutoDock v4.0. The X-ray crystal structure of XO/salicylic acid complex from bovine milk (PDB code: 1N5X) was obtained from RCSB Protein Database Bank. The 3D structures of small molecules were generated by Chem3D Ultra 14.0. The rotatable bonds of ligands were detected and assigned with Auto Dock tools. The protein was prepared by repairing the missing and terminal residues of polypeptide chains, deleting water, assigning atom types and adding hydrogen atoms. All the other miscellaneous parameters were set as default. The docked model with the lowest binding energy and highest percentage frequency was chosen to represent the most favorable binding mode as predicted by the program. The output from AutoDock was rendered with PyMOL for the graphic display.

Acknowledgments

This project was supported in part by the Applied Basic Research Project of Yunnan Province (No.2016FA030) and the National Natural Science Foundation of China (31370377). The authors are grateful to Dr Johann Schinnerl, University of Vienna, for his language editing.

References

Aimi, N., Yamanaka, E., Shinma, N., Fujiu, M., Kurita, J., Sakai, S., Haginiwa, J., 1977. Studies on plants containing indole alkaloids. VI Minor bases of *Uncaria rhynchophylla* Miq. Chem. Pharm. Bull. 25, 2067–2071.
Ahond, A., Bui, A.M., Potier, P., Hagaman, E.W., Wenkert, E., 1976. Carbon-13 nuclear magnetic resonance analysis of vobasine-like indole alkaloids. J. Org. Chem. 41, 1878–1879.
Al-Shamma, A., Drake, S., Flynn, D.L., Mitscher, L.A., Park, Y.H., Rao, G.S.R., Simpson, A., Swayze, J.K., Veysoglu, T., Wu, S.T.S., 1981. Antimicrobial agents from higher plants. Antimicrobial agents from *Peganum harmala* seeds. J. Nat. Prod. 44, 745–747.
Atta-ur-Rahaman, Habib-ur-Rehman, 1986. Isolation and NMR studies on rhazimal and strictamine. Planta Med. 52, 230–231.
Atta-ur-Rahaman, Pervin, A., Muzaffar, A., De Silva, K.T.D., Silva, W.S.J., 1989. Alkaloids of *Petchia ceylanica*. Phytochemistry 28, 3221–3225.
Baassou, S., Mehri, H., Plat, M., 1978. Plants of New Caledonia. Part 49. Alkaloids of Melodinus aeneus. Phytochemistry 17, 1449–1450.
Bach, M.H., Simkin, P.A., 2014. Uricosuric drugs: the once and future therapy for hyperuricemia? Curr. Opin. Rheumatol. 26, 169–175.
Bailleul, F., Delaveau, P., Rabaron, A., Plat, M., Koch, M., 1977. Feretoside et gardenoside du *Feretia apodanthera*: NMR du carbon 13 en serie iridoide. Phytochemistry 16, 723–726.
Bari, L.D., Pescitelli, G., Pratelli, C., Pini, D., Salvadori, P., 2001. Determination of absolute configuration of acyclic 1,2-diols with $Mo_2(OAc)_4$. 1. Snatzke's Method Revisited. J. Org. Chem. 66, 4819–4825.
Boughandjioua, N., Bengaouer, L., Hotellier, F., Seguin, E., Tillequin, F., Koch, M., Sevenet, T., 1989. Alkaloids of *Ochrosia alyxioides*. J. Nat. Prod. 52, 1107–1112.
Bruce, S.P., 2006. Febuxostat: a selective xanthine oxidase inhibitor for the treatment of hyperuricemia and gout. Ann. Pharmacother. 40, 2187–2194.
Cai, X.H., Bao, M.F., Zhang, Y., Zeng, C.X., Liu, Y.P., Luo, X.D., 2011. A new type of monoterpenoid indole alkaloid precursor from *Alstonia rostrata*. Org. Lett. 13, 3568–3571.
Chen, C.Y., Chang, F.R., Wu, Y.C., 1997. The constituents from the stems of *Annona cherimola*. J. Chin. Chem. Soc. 44, 313–319.
Clivio, P., Richard, B., Hadi, H.A., David, B., Sevenet, T., Zeches, M., Le Men-Olivier, L., 1990. Alkaloids from leaves and stem bark of *Ervatamia polyneura*. Phytochemistry 29, 3007–3011.
Delgado, J.N., Cosgrove, F.P., Isaacson, E.I., 1966. Allopurinol: xanthine oxidase inhibitor. Tex. Med. 62, 100–101.
Eles, J., Kalaus, G., Greiner, I., Peredy, M.K., Szabo, P., Keseru, G.M., Szabo, L., Szantay, C., 2002. Synthesis of *Vinca* alkaloids and related compounds. 100. stereoselective oxidation reactions of compounds with the aspidospermane and quebrachamine ring system. First synthesis of some alkaloids containing the epoxy ring. J. Org. Chem. 67, 7255–7260.
Feng, X.Z., Kan, C., Husson, H.P., Potier, P., Kan, S.K., Lounasmaa, M., 1981. New dimeric indole alkaloids of the voacamine type extracted from *Ervatamia hainanensis*. J. Nat. Prod. 44, 670–675.
Feng, X.Z., Kan, C., Potier, P., Kan, S.K., Lounasmaa, M., 1982. Monomeric indole alkaloids from *Ervatamia hainanensis*. Planta Med. 44, 212–214.
Greig, S.L., Garnock-Jones, K.P., 2016. Loxoprofen: a review in pain and inflammation. Clin. Drug Investig. 36, 771–781.
Gunasekera, S.P., Cordell, G.A., Farnsworth, N.R., 1980. Anticancer indole alkaloids of *Ervatamia heyneana*. Phytochemistry 19, 1213–1218.
Hamonniere, M., Leboeuf, M., Cave, A., 1977. Alkaloids from Annonaceae. Part 15. Aporphine alkaloids and terpenoid compounds from *Polyalthia oliveri*. Phytochemistry 16, 1029–1034.
Höfle, G., Heinstein, P., Stöckigt, J., Zenk, M.H., 1980. ^1H-NMR analysis of ajmalicine–type alkaloids of the 3α series. Planta Med. 40, 120–126.
Hu, W.L., Zhu, J.P., Piantini, U., Prewo, R., Hesse, M., 1987. Revision of the structures of rhazicine and rhazimine, two alkaloids from *Melodinus acutiflorus*. Phytochemistry 26, 2625–2630.
Kalaus, G., Greiner, I., Kajtar-Peredy, M., Brlik, J., Szabo, L., Szantay, C., 1993. Synthesis of vinca alkaloids and related compounds. 64. Total syntheses of (±) -pseudovincadifformine and (±) -20-epipseudovincadifformine. J. Org. Chem. 58, 6076–6082.
Kam, T.S., Loh, K.Y., Chen, W., 1993. Conophylline and conophyllidine: new dimeric alkaloids from *Tabernaemontana divaricata*. J. Nat. Prod. 56, 1865–1871.
Kam, T.S., Pang, H.S., Choo, Y.M., Komiyama, K., 2004. Biologically active ibogan and vallesamine derivatives from *Tabernaemontana divaricata*. Chem. Biodivers. 1, 646–656.
Kam, T.S., Pang, H.S., Lim, T.M., 2003. Biologically active indole and bisindole alkaloids from *Tabernaemontana divaricata*. Org. Biomol. Chem. 1, 1292–1297.
Kam, T.S., Sim, K.M., 2002. Five new iboga alkaloids from *Tabernaemontana corymbosa*. J. Nat. Prod. 65, 669–672.
Kam, T.S., Sim, K.M., 2003. Conodurine, conoduramine, and ervahanine derivatives from *Tabernaemontana corymbosa*. Phytochemistry 63, 625–629.
Kan, C., Husson, H.P., Kan, S.K., Lounasmaa, M., 1981. Determination of structures by proton NMR at 400 MHz: two new alkaloids from *Tabernaemontana albiflora*. Planta Med. 41, 195–197.
Krishnamurthy, B., Rani, N., Bharti, S., Golechha, M., Bhatia, J., Nag, T.C., Ray, R., Arava, S., Arava, S.D., 2015. Febuxostat ameliorates doxorubicin-induced cardiotoxicity in rats. Chem. Biol. Interact. 237, 96–103.
Kunesch, N., Tulinsky, A., 1967. Voacanga alkaloids. VII. Structure of voaphylline. Bull. Soc. Chim. Fr. 6, 2155–2160.
Kutney, J.P., Brown, R.T., 1966. Structural elucidation of sitsirikine dihydrositsirikine

and isositsirikine-3. New alkaloids from *Vinca rosea* Linn. Tetrahedron 22, 321–336.
Kutney, J.P., Honda, T., Joshua, A.V., Lewis, N.G., Worth, B.R., 1978. Total synthesis of indole and dihydroindole alkaloids. XIII. Further chemistry of catharanthine. Helv. Chim. Acta 61, 690–700.
Le Men, J.G., Hoizey, M.J., Lukacs, G., Le Men-Olivier, L., Levy, J., 1974. Structure of pandine, a hexacyclic alkaloid of the ψ-vincadifformine type. Tetrahedron Lett. 36, 3119–3122.
Leonard, N.J., Elderfield, R.C., 1942. Alstonia alkaloids. I. Degradation of alstonine to β-carboline bases and the reduction of tetrahydroalstonine with sodium and butyl alcohol. J. Org. Chem. 7, 556–572.
Lim, K.H., Hiraku, O., Komiyama, K., Koyano, T., Hayashi, M., Kam, T.S., 2007. Biologically active indole alkaloids from *Kopsia arborea*. J. Nat. Prod. 70, 1302–1307.
Matsui, M., Kabashima, T., Ishida, K., Takebayashi, T., Watanabe, Y., 1982. Studies on the alkaloids of menispermaceous plants. 274. Alkaloids of the leaves of *Stephania japonica*. J. Nat. Prod. 45, 497–500.
Mehmood, A., Ishaq, M., Zhao, L., Safdar, B., Ashfaq-ur, R., Muni, M., Raza, A., Nadeem, M., Iqbal, W., Wang, C., 2019. Natural compounds with xanthine oxidase inhibitory activity: a review. Chem. Biol. Drug Des. 93, 387–418.
Monique, Z.H., Jean-Marc, N., Bernard, R., Hubert, S., Hamid, A.H., Thierry, S., Louisette, L.O., 1995. Alkaloids from leaves and stem bark of *Ervatamia peduncularis*. Phytochemistry 40, 587–591.
Mollov, N.M., Le, N.T., 1971. Thalmelatidine, a new aporphine-benzylisoquinoline alkaloid from the roots of *Thalictrum minum* subspecies elatum. Dokl. Bulg. Acad. Nauk. 24, 601–604.
Mors, W.B., Zaltzman, P., Beereboom, J.J., Pakrashi, S.C., Djerassi, C., 1956. Alkaloids of two Brazilian Apocynaceae: *Rauwolfia grandiflora* and *Lochnera* (*Vinca*) *rosea* var. *alba*. Chem. Ind. 75, 173–174.
Okuyama, E., Gao, L.H., Yamazaki, M., 1992. Analgesic components from bornean medicinal plants, *Tabernaemontana pauciflora* blume and *Tabernaemontana pandacaqui* poir. Chem. Pharm. Bull. 40, 2075–2079.
Pacher, P., Nivorozhkin, A., Szabo, C., 2006. Therapeutic effects of xanthine oxidase inhibitors: renaissance half a century after the discovery of allopurinol. Pharmacol. Rev. 58, 87–114.
Pascart, T., Richette, P., 2018. Colchicine in gout: an update. Curr. Pharmaceut. Des. 24, 684–689.
Pereira, P.S., Franca, S.D.C., Oliveira, P.V.A.D., Breves, C.M.D.S., Pereira, S.I.V., 2008. Chemical constituents from *Tabernaemontana catharinensis* root bark: a brief NMR review of indole alkaloids and in vitro cytotoxicity. Quim. Nova 31, 20–24.
Perera, P., Sandberg, F., Van Beek, T.A., Verpoorte, R., 1984. Tertiary indole alkaloids from fruits of *Tabernaemontana dichotoma*. Planta Med. 50, 251–252.
Perera, P., Sandberg, F., Van Beek, T.A., Verpoorte, R., 1985. Alkaloids of stem and rootbark of *Tabernaemontana dichotoma*. Phytochemistry 24, 2097–2104.
Rastogi, K., Kapil, R.S., Popli, S.P., 1980. New alkaloids from *Tabernaemontana divaricata*. Phytochemistry 19, 1209–1212.
Schripsema, J., Hermans-Lokkerbol, A., Van der Heijden, R., Verpoorte, R., Svendsen, A.B., Van Beek, T.A., 1986. Pharmacognostical studies of *Tabernaemontana* species. Part 18. Alkaloids of *Tabernaemontana ventricosa*. J. Nat. Prod. 49, 733–735.
Sharma, P., Cordell, G.A., 1988. Heyneanine hydroxyindolenine, a new indole alkaloid from *Ervatamia coronaria* var. *plena*. J. Nat. Prod. 51, 528–531.
Subramaniam, G., Hiraku, O., Hayashi, M., Koyano, T., Komiyama, K., Kam, T.S., 2007. Biologically active aspidofractinine, rhazinilam, akuammiline, and vincorine alkaloids from *Kopsia*. J. Nat. Prod. 70, 1783–1789.
Van Beek, T.A., Verpoorte, R., Svendsen, A.B., 1984. Isolation and synthesis of vobparicine, a novel type dimeric indole alkaloid. Tetrahedron Lett. 25, 2057–2060.
Waterman, P.G., Zhong, S., 1982. Vallesiachotamine and isovallesiachotamine from the seeds of *Strychnos tricalysioides*. Planta Med. 45, 28–30.
Wenkert, E., Hagaman, E.W., Kunesch, N., Wang, N.Y., Zsadon, B., 1976. Carbon-13 NMR spectroscopy of naturally occurring substances. XLII. Conformational analysis of quebrachamine-like indole alkaloids and related substances. Helv. Chim. Acta 59, 2711–2723.
Wenkert, E., Hagaman, E.W., Wang, N.Y., Kunesch, N., 1979. The C(7) stereochemistry of the chloroindolenines of cleavamines and quebrachamines. Heterocycles 12, 1439–1443.
Ying, Y.M., Shan, W.G., Liu, W.H., Zhan, Z.J., 2013. Alkaloids and nucleoside derivatives from a fungal endophyte of *Huperzia serrata*. Chem. Nat. Compd. 49, 184–186.
Yu, J.M., Wang, T., Liu, X.X., Deschamps, J., Flippen-Anderson, J., Liao, X.B., Cook, J.M., 2003. General approach for the synthesis of sarpagine indole alkaloids. Enantiospecific total synthesis of (+)-vellosimine, (+)-normacusine B, (-)-alkaloid Q3, (-)-panarine, (+)-Na-methylvellosimine, and (+)-Na-methyl-16-epipericyclivine. J. Org. Chem. 68, 7565–7581.
Zhang, B.J., Teng, X.F., Bao, M.F., Zhong, X.H., Ni, L., Cai, X.H., 2015a. Cytotoxic indole alkaloids from *Tabernaemontana officinalis*. Phytochemistry 120, 46–52.
Zhang, B.J., Liu, C., Bao, M.F., Zhong, X.H., Ni, L., Wu, J., Cai, X.H., 2017. Novel monoterpenoid indole alkaloids from *Melodinus yunnanensis*. Tetrahedron 73, 5821–5826.
Zhang, D.B., Yu, D.G., Sun, M., Zhu, X.X., Yao, X.J., Zhou, S.Y., Chen, J.J., Gao, K., 2015b. Ervatamines A-I, anti-inflammatory monoterpenoid indole alkaloids with diverse skeletons from *Ervatamia hainanensis*. J. Nat. Prod. 78, 1253–1261.
Zhang, G.L., Ruecker, G., Breitmaier, E., Mayer, R., Steinbeck, C., 1998. Alkaloids from *Thalictrum przewalskii*. Planta Med. 64, 165–171.
Zhang, H., Wang, X.N., Lin, L.P., Ding, J., Yue, J.M., 2007. Indole alkaloids from three species of the *ervatamia* Genus: *E. officinalis*, *E. divaricata*, and *E. divaricata* gouyahua. J. Nat. Prod. 70, 54–59.
Zhang, Y.W., Yang, R., Cheng, Q., Ofuji, K., 2003. Henrycinols A and B, two novel indole alkaloids isolated from *Melodinus henryi* Craib. Helv. Chim. Acta 86, 415–419.
Zhou, C.J., Guan, H.Y., Zhang, Y.H., Xu, R., Hao, X.J., Yang, X.S., 2012. Alkaloids in *Melodinus fusiformis*. Zhongchengyao 34, 85–89.